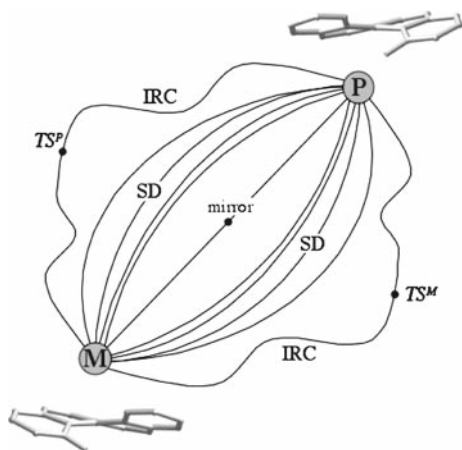


# Narcissistic reaction pathways: an example of Maxwell's theorem of geometrical optics applied to the intrinsic reaction coordinate model

Miquel Llunell · Pere Alemany · Josep Maria Bofill

Received: 6 June 2008 / Accepted: 8 August 2008 / Published online: 9 September 2008  
© Springer-Verlag 2008

**Abstract** Maxwell's theorem and the concept of stigmatic transformations that appear in the theory of geometrical optics are extended to the intrinsic reaction coordinate model when it is applied to the specific case of narcissistic reactions.



**Keywords** Reaction path · Narcissistic reaction · Chirality measures · Chiral path · Helicenes

M. Llunell (✉) · P. Alemany  
Departament de Química Física, Institut de Química Teòrica i Computacional (IQTC), Universitat de Barcelona,  
Martí i Franquès, 1-11, 08028 Barcelona, Catalonia, Spain  
e-mail: llunell@ub.edu

J. M. Bofill  
Departament de Química Orgànica, Institut de Química Teòrica i Computacional (IQTC), Universitat de Barcelona,  
Martí i Franquès, 1-11, 08028 Barcelona, Catalonia, Spain

## 1 Introduction

Mirrors are the oldest optical devices known by humanity. The simplest case is a planar mirror; this device creates images of objects lying in front of it. These images appear to be behind the plane in which the mirror lies. A close inspection shows that the mirror image has the same size as the original object, yet is different from it unless the object has reflection symmetry. The relation between an object and its image reflected on a planar mirror is well known and satisfactorily described within the theory of geometrical or ray optics.

In chemistry, enantiomers of a molecular structure are stereoisomers that are nonsuperimposable complete mirror images of each other. From the development of a coherent theory of stereochemistry, the general relation between enantiomeric molecular structures has been the object of particular attention [1]. The study of enantiomerization pathways, that is the paths of reactions, which take us from a given molecular structure to that of its enantiomer, has a crucial importance in many processes of molecular synthesis. Reactions in which their mechanisms can be described as a pure reflection between reactants and products were termed by Salem as “narcissistic reactions” [2]. Salem in his original work distinguished between two possible types of pathways for a narcissistic reaction. In a synchronous path, the reaction proceeds “through the mirror relating both enantiomers” with a single point of the path lying exactly on this mirror. For an enantiomerization, this path is termed achiral, since it necessarily contains at least one achiral point (the point on the mirror). On the other hand, the process can proceed through one of the pair of paths “around the mirror.” In this case, there is the possibility of enantiomerization through a chiral path, that is, a path joining two enantiomers for which all points represent chiral structures.

In the present letter, we analyze the features of both synchronous and nonsynchronous processes for narcissistic reactions using the model of the intrinsic reaction coordinate (IRC) to describe its reaction path. Since the IRC paths possess a variational nature [3] like that of light rays in geometrical optics (GO), we will use this analogy to show that the IRCs describing the mechanism of narcissistic nonsynchronous reactions must necessarily satisfy a relation equivalent to that given in Maxwell's theorem of GO. In the present context and throughout the article, the meaning of "variational nature" of a curve is that it makes stationary the value of an integral evaluated along this curve. In optics, it is possible to find transformations that transform all light rays starting at a given point into light rays that pass through the image of the original point. This kind of transformations is called stigmatic, and Maxwell showed that every stigmatic transformation is trivial in the sense that both the object and its image have the same size. As a matter of fact, the planar mirror is the only optical instrument that is known to produce a stigmatic transformation [4]. We will show in the following section that, if the pathways for a narcissistic reaction are nonsynchronous and can be described by the IRC model, it is possible to find a mathematical transformation with the same behavior of stigmatic transformations in optics satisfying the Maxwell's theorem.

## 2 Formulation of Maxwell's theorem in the context of the intrinsic reaction coordinate model

In geometric or ray optics, light propagation is described in terms of rays. A ray in GO is an abstract object that is perpendicular to the wavefronts of the actual optical waves. Rays are bent at the interface between two dissimilar media, and in the general case, they may be curved in an anisotropic medium in which the refractive index is a continuous function of position. The basic law describing the processes in GO is Fermat's principle, also known as the principle of least time, which states that the path taken between two points by a ray of light is the path that can be traversed in least time.

From a mathematical point of view, light rays are extremals of a variational problem: a ray of light starting at a point  $\mathbf{x}(t_0)$  and ending at a point  $\mathbf{x}(t)$  has the property of minimizing the time required to travel along a regular curve  $C$  that joins these two points. If we consider that the light rays travel through an anisotropic medium, Fermat's principle is formulated mathematically as a stationary path of the following expression:

$$I(\mathbf{x}, \mathbf{x}_0) = \int_{t_0}^t F(\mathbf{x}_C, \dot{\mathbf{x}}_C) dt' = \int_{t_0}^t f(\mathbf{x}_C) \sqrt{\dot{\mathbf{x}}_C^T \dot{\mathbf{x}}_C} dt' \quad (1)$$

where  $I(\mathbf{x}, \mathbf{x}_0)$  is the time needed by the light ray to travel from point  $\mathbf{x}_0 = \mathbf{x}_C(t_0)$  to point  $\mathbf{x} = \mathbf{x}_C(t)$ ,  $\mathbf{x}_C$  an arbitrary point on the path  $C$  followed by the ray,  $f(\mathbf{x}_C)$  the refraction index at this point and  $(\dot{\mathbf{x}}_C^T \dot{\mathbf{x}}_C)^{1/2} dt' = ds$  the differential of arc length of the ray.

One of the principal applications of GO is the design of optical instruments where light waves are processed to enhance an image for viewing. In an optical instrument, an incident ray following a path  $\mathbf{x}_C$  is transformed in an image ray described by a path  $\mathbf{x}_C^I$ . In this context, one of the main problems in the design of optical instruments consists in finding transformations that yield a sharp image of an observed object. A transformation that satisfies this requirement is said to be *stigmatic* and an optical instrument that produces a stigmatic transformation is called an absolute instrument. A result from Maxwell proves that for any stigmatic transformation the resulting mapping is trivial, which means that the object and its image have the same size. This condition is satisfied when the optical length (or travel time) of a ray curve,  $I(\mathbf{x}, \mathbf{x}_0)$ , and that of its image curve,  $I(\mathbf{x}^I, \mathbf{x}_0^I)$ , are exactly the same. If we consider the particular case where the refraction index,  $f(\mathbf{x}_C)$ , is constant along a ray curve and its image curve, as would be the case for a mapping through a lens system with air at both sides, then their optical lengths coincide, which is an example of Maxwell's theorem. An important case for the discussion below is a plane mirror, which can be shown to be an optical instrument producing stigmatic transformations.

Let us now move to the description of chemical reactions and translate the above results of GO to the reaction path model. For a chemical reaction, the reaction path (RP) or minimum energy path (MEP) is a curve located on an  $N$ -dimensional potential energy surface (PES) [5]. An usual procedure to describe the MEP between two minima on the PES is to locate first a transition structure connecting both minima and then find the intrinsic reaction coordinate (IRC) paths, defined as the steepest descent (SD) curves connecting a first-order saddle point (the transition structure) with a stationary point of character minimum (corresponding to either reactants or products). From a mathematical point of view, a SD curve can be defined as the curve that extremalizes the integral functional given in Eq. 1 where now  $t$ , the parameter that characterizes the arbitrary curve  $C$ , is the so-called reaction coordinate,  $\mathbf{x} = \mathbf{x}_C(t)$  and  $\mathbf{x}_0 = \mathbf{x}_C(t_0)$  are two points on the  $N$ -dimensional PES  $V(\mathbf{x})$ , connected by curve  $C$ ,  $\dot{\mathbf{x}}_C = d\mathbf{x}_C/dt'$  is the tangent vector of this curve at the point  $\mathbf{x}_C(t')$ , and  $f(\mathbf{x}_C) = (\mathbf{g}^T(\mathbf{x}_C)\mathbf{g}(\mathbf{x}_C))^{1/2}$ , with  $\mathbf{g}(\mathbf{x}') = \nabla_{\mathbf{x}} V(\mathbf{x})|_{\mathbf{x}=\mathbf{x}'}$  is the energy gradient with respect to the  $\mathbf{x}$  coordinates at the point  $\mathbf{x}'$ , and the operator  $\nabla_{\mathbf{x}}^T = (\partial/\partial x_1, \dots, \partial/\partial x_N)$  [6]. By construction, for any point on an SD curve,  $\dot{\mathbf{x}}_{SD} = \nabla_{\mathbf{x}} V(\mathbf{x}_{SD})$

must hold. The function  $f(\mathbf{x}_C) = (\mathbf{g}^T(\mathbf{x}_C)\mathbf{g}(\mathbf{x}_C))^{1/2}$  represents the speed law for the curve  $C$  propagating through the PES  $V(\mathbf{x})$ .

Let us recall that the IRC path is just a particular SD curve that passes through a first-order saddle point. So, while there are infinite SD curves departing from a given minimum on the PES, it can be shown that there is only one of those reaching the transition structure. On the other hand, since the integral functional (Eq. 1) defining the SD curves has the same mathematical structure as that describing the propagation of light rays in the theory of GO, we can interpret the SD curves, and in particular the IRC paths, as light rays moving through an anisotropic medium with variable “index of refraction,”  $f(\mathbf{x})$ . It can be shown that the set of extremal curves of integral (Eq. 1) with the same origin,  $\mathbf{x}_0$ , cuts transversally (in this case transversality is equivalent to orthogonality) a set of contour lines with constant potential energy,  $V(\mathbf{x}) = \text{constant}$ . This behavior is equivalent to the Fermat–Huyghens principle in the construction of wave fronts for the propagation of light [6]. In this analogy between GO and the IRC model, the light rays correspond to the SD paths, the  $t$  parameter is the arc length for the ray path and the reaction coordinate for the SD path, and the value of the integral  $I(\mathbf{x}, \mathbf{x}_0)$  is the time of propagation for the light rays and the change in potential energy for SD curves on a PES.

The mathematical analogy between both models, GO and IRC, opens the question of the possible application of stigmatic transformations and Maxwell’s theorem [4] to narcissistic reactions [2], a particular case of chemical reactions that are equivalent to a pure reflection in a fixed mirror plane. Narcissistic reactions cover, but are not restricted to, the vast majority of enantiomerizations. Exceptions are those enantiomerization reactions in which reactants and products are related by an  $S_n$  axis. The family of narcissistic reactions includes also a wide variety of automerizations such as the Cope rearrangement. Although in certain cases the mirror plane relating reactants and products coincides with a symmetry plane of the reactants (or products), this is not a necessary condition.

To apply the concepts described above to a narcissistic reaction, let us consider an IRC path  $\mathbf{x}_{\text{IRC}}(t')$ , which connects the points  $\mathbf{x}_0 = \mathbf{x}_{\text{IRC}}(t_0)$  associated to the reactant and  $\mathbf{x}_{\text{TS}} = \mathbf{x}_{\text{IRC}}(t_{\text{TS}})$  associated to a first-order saddle point (Figs. 1, 2). For a narcissistic reaction, as stated above, the minimum energy configuration associated to products  $\mathbf{x}_0^{\text{I}}$  is related to that of the reactants  $\mathbf{x}_0$  by a reflection in a fixed mirror plane. Let us define the path joining the transition state with the product configuration as the image of the IRC path,  $\mathbf{x}_{\text{IRC}}^{\text{I}}(t')$ . As discussed by Salem [2], there are two possibilities for narcissistic reactions. If there is a single transition state joining reactants and products, the reaction is said to proceed via a synchronous process (Fig. 1). If, on

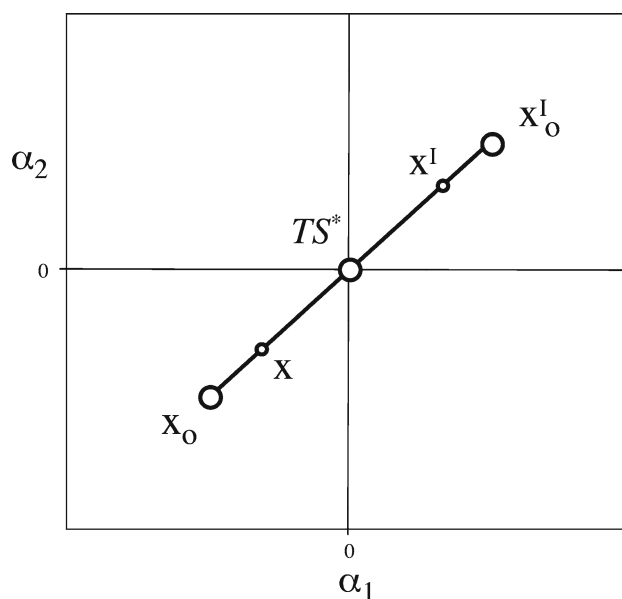


**Fig. 1** The IRC path for a synchronous enantiomerization process projected in the two-dimensional space defined by two antisymmetric coordinates ( $\alpha_1$  and  $\alpha_2$ ). The line indicates the IRC curve connecting the two points  $\mathbf{x}_0$  and  $\mathbf{x}_0^{\text{I}}$ , corresponding to reactants and products. A general point at the path and its mirror image ( $\mathbf{x}$  and  $\mathbf{x}^{\text{I}}$ ) and the achiral transition state ( $\text{TS}^*$ ) are also indicated

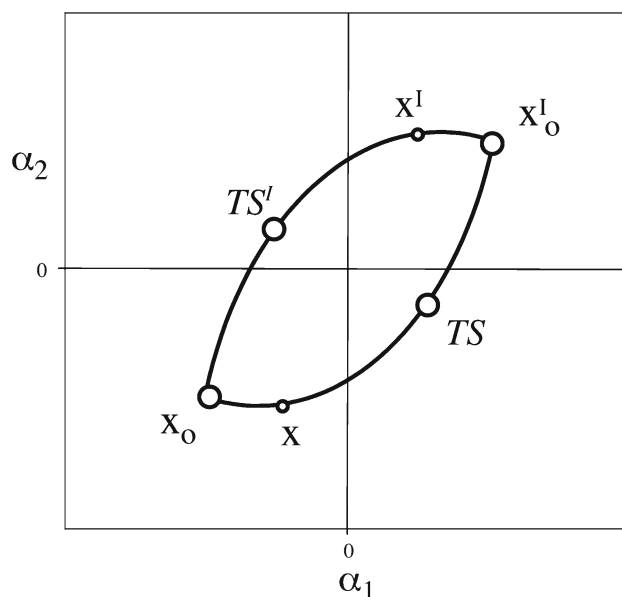


**Fig. 2** The IRC paths for a nonsynchronous enantiomerization process projected in the two-dimensional space defined by two antisymmetric coordinates ( $\alpha_1$  and  $\alpha_2$ ). The lines indicate the IRC curves connecting the points  $\mathbf{x}_0$  and  $\mathbf{x}_0^{\text{I}}$ , corresponding to reactants and products. A general point ( $\mathbf{x}$  and  $\mathbf{x}^{\text{I}}$ ) and the enantiomeric transition states ( $\text{TS}$  and  $\text{TS}^{\text{I}}$ ) are also indicated

the contrary, there are two independent, but symmetry-related, pathways joining reactants and products with two distinct, but symmetry-related, transition states, the process is said to be nonsynchronous (Fig. 2). Notice that for a

narcissistic reaction the end point of each IRC curve,  $\mathbf{x}_{\text{IRC}}(t_f)$ , must coincide with the image of its starting point:  $\mathbf{x}_{\text{IRC}}(t_f) = \mathbf{x}_0^{\text{I}}$ .

Let us now assume that it is possible to find a stigmatic transformation from a point  $\mathbf{x}_{\text{IRC}}$  to a point  $\mathbf{x}_{\text{IRC}}^{\text{I}}$ . In this case, the coordinates  $\mathbf{x}_{\text{IRC}}$  and  $\mathbf{x}_{\text{IRC}}^{\text{I}}$  are related through  $\mathbf{x}_{\text{IRC}}^{\text{I}} = \mathbf{q}(\mathbf{x}_{\text{IRC}})$ , with  $\mathbf{q}$  being a transformation function which is assumed to have the inverse form. According to the theory of calculus of variations (CV) [7], the value of integral (Eq. 1) evaluated on an extremal curve, in the present case either the  $\mathbf{x}_{\text{IRC}}$  or  $\mathbf{x}_{\text{IRC}}^{\text{I}}$  paths, equals the value of the integral evaluated on a total differential form:

$$\begin{aligned} \int_{t_0}^t F(\mathbf{x}_{\text{IRC}}, \dot{\mathbf{x}}_{\text{IRC}}) dt' &= \int_{t_0}^t \nabla_{\dot{\mathbf{x}}}^T(F(\mathbf{x}_{\text{IRC}}, \dot{\mathbf{x}}_{\text{IRC}})) \dot{\mathbf{x}}_{\text{IRC}} dt' \\ &= \int_{t_0}^t \mathbf{g}^T(\mathbf{x}_{\text{IRC}}) \dot{\mathbf{x}}_{\text{IRC}} dt' = \int_{t_0}^t \nabla_{\mathbf{x}}^T(V(\mathbf{x}_{\text{IRC}})) \dot{\mathbf{x}}_{\text{IRC}} dt' \\ &= \int_{\mathbf{x}_0}^{\mathbf{x}} \nabla_{\mathbf{x}}^T(V(\mathbf{x}_{\text{IRC}})) d\mathbf{x}_{\text{IRC}} \end{aligned} \quad (2)$$

where  $\nabla_{\dot{\mathbf{x}}} F(\mathbf{x}_{\text{IRC}}, \dot{\mathbf{x}}_{\text{IRC}}) = \mathbf{g}(\mathbf{x}_{\text{IRC}}) = \nabla_{\mathbf{x}} V(\mathbf{x}_{\text{IRC}})$  is needed in order to construct the differential form as required. Since in equality (Eq. 2) the last integral does not depend on the choice of the curve joining the points  $\mathbf{x}_0$  and  $\mathbf{x}$ , and  $\mathbf{x}_0$  is a fixed point, then it is only a function of the final point  $\mathbf{x}$ , and we can write,

$$\begin{aligned} \int_{\mathbf{x}_0}^{\mathbf{x}} \nabla_{\mathbf{x}}^T(V(\mathbf{x}_{\text{IRC}})) d\mathbf{x}_{\text{IRC}} &= \int_{\mathbf{x}_0}^{\mathbf{x}} \nabla_{\mathbf{x}}^T(V(\mathbf{x}_A)) d\mathbf{x}_A \\ &= \int_{\mathbf{x}_0}^{\mathbf{x}} \mathbf{g}^T(\mathbf{x}_A) d\mathbf{x}_A = \int_{v_0}^v dV = v - v_0 \end{aligned} \quad (3)$$

with  $v = V(\mathbf{x})$  and  $v_0 = V(\mathbf{x}_0)$ . In this expression, the second integral is evaluated along an arbitrary path,  $\mathbf{x}_A(t')$ , embedded on the PES and joining points  $\mathbf{x}_0$  and  $\mathbf{x}$  as the IRC curve does. From a geometrical point of view, Eq. 3 means that at each point of the IRC curve it transverses orthogonally the family of contour lines,  $V(\mathbf{x}) = \text{constant}$  [6]. Proceeding in the same way for the transformed IRC path we arrive to

$$\int_{t_0}^t F(\mathbf{x}_{\text{IRC}}^{\text{I}}, \dot{\mathbf{x}}_{\text{IRC}}^{\text{I}}) dt' = \int_{v_0^{\text{I}}}^{v^{\text{I}}} dV = v^{\text{I}} - v_0^{\text{I}} \quad (4)$$

where  $v^{\text{I}} = V(\mathbf{x}^{\text{I}})$  and  $v_0^{\text{I}} = V(\mathbf{x}_0^{\text{I}})$ . From all the considerations above we say that the reactant point,  $\mathbf{x}_0$ , and the

product point,  $\mathbf{x}_0^{\text{I}}$ , which is the mirror image of the reactant point in a narcissistic reaction, are conjugate points. In other words, integral (Eq. 1) evaluated along any extremal curve, either IRC or SD, connecting points,  $\mathbf{x}_0$  and  $\mathbf{x}_0^{\text{I}}$  has the same value.

The transformation  $\mathbf{x}_{\text{IRC}}^{\text{I}} = \mathbf{q}(\mathbf{x}_{\text{IRC}})$  should satisfy the requirement that both curves,  $\mathbf{x}_{\text{IRC}}$  and  $\mathbf{x}_{\text{IRC}}^{\text{I}}$ , transverse orthogonally the family of contour lines,  $V(\mathbf{x}) = \text{constant}$ , belonging to the PES, and this behavior is achieved if the next set of equalities is satisfied

$$\begin{aligned} \int_{t_0}^t F(\mathbf{x}_{\text{IRC}}^{\text{I}}, \dot{\mathbf{x}}_{\text{IRC}}^{\text{I}}) dt' - \int_{t_0}^t F(\mathbf{x}_{\text{IRC}}, \dot{\mathbf{x}}_{\text{IRC}}) dt' \\ = \int_{t_0}^t \mathbf{g}^T(\mathbf{x}_{\text{IRC}}^{\text{I}}) \dot{\mathbf{x}}_{\text{IRC}}^{\text{I}} dt' - \int_{t_0}^t \mathbf{g}^T(\mathbf{x}_{\text{IRC}}) \dot{\mathbf{x}}_{\text{IRC}} dt' \end{aligned} \quad (5a)$$

since the two first integrals are evaluated along the IRC paths, their values coincide with the value of the integrals computed along a total differential form. Now, we substitute the derivative with respect to  $t$  of the transformation  $\mathbf{x}_{\text{IRC}}^{\text{I}} = \mathbf{q}(\mathbf{x}_{\text{IRC}})$  in the first integrand of the right hand side part of Eq. 5a

$$\begin{aligned} \int_{t_0}^t \mathbf{g}^T(\mathbf{x}_{\text{IRC}}^{\text{I}}) (\nabla_{\mathbf{x}} \mathbf{q}^T(\mathbf{x}_{\text{IRC}})) \dot{\mathbf{x}}_{\text{IRC}} dt' - \int_{t_0}^t \mathbf{g}^T(\mathbf{x}_{\text{IRC}}) \dot{\mathbf{x}}_{\text{IRC}} dt' \\ = \int_{\mathbf{x}_0}^{\mathbf{x}} [\mathbf{g}^T(\mathbf{x}_{\text{IRC}}^{\text{I}}) (\nabla_{\mathbf{x}} \mathbf{q}^T(\mathbf{x}_{\text{IRC}})) - \mathbf{g}^T(\mathbf{x}_{\text{IRC}})] d\mathbf{x}_{\text{IRC}} \end{aligned} \quad (5b)$$

the first term within brackets of the integrand of the right hand side part of Eq. 5b is the transformation of  $\mathbf{g}(\mathbf{x}_{\text{IRC}})$  to the new coordinates. Finally, the last integrand can be written as

$$\begin{aligned} \int_{\mathbf{x}_0}^{\mathbf{x}} \nabla_{\mathbf{x}}^T W(\mathbf{x}_{\text{IRC}}) d\mathbf{x}_{\text{IRC}} &= \int_{t_0}^t \nabla_{\mathbf{x}}^T W(\mathbf{x}_{\text{IRC}}) \dot{\mathbf{x}}_{\text{IRC}} dt' \\ &= \int_{t_0}^t (dW(\mathbf{x}_A)/dt') dt' \\ &= \int_{W_0}^{W(\mathbf{x})} dW = W(\mathbf{x}) - W_0 = (v^{\text{I}} - v_0^{\text{I}}) - (v - v_0) \end{aligned} \quad (5c)$$

where  $W(\mathbf{x})$  is a function such that  $dW(\mathbf{x})/dt$  is a total derivative, since in this way the last integral does not depend on the curve that is chosen for integration, which implies that the last equality is satisfied. In other words, the transversality condition is fulfilled. If we differentiate  $W(\mathbf{x})$  in Eq. 5 with respect to  $t'$  at  $t' = t$ , we have

$$\begin{aligned}
 \frac{d}{dt} W(\mathbf{x}) &= \nabla_{\mathbf{x}}(W(\mathbf{x}))^T \dot{\mathbf{x}} \\
 &= f(\mathbf{q}(\mathbf{x})) \sqrt{(\dot{\mathbf{x}}^I)^T (\dot{\mathbf{x}}^I)} - f(\mathbf{x}) \sqrt{\dot{\mathbf{x}}^T \dot{\mathbf{x}}} \\
 &= f(\mathbf{q}(\mathbf{x})) \sqrt{\dot{\mathbf{x}}^T [\nabla_{\mathbf{x}}(\mathbf{q}(\mathbf{x}))^T]^T [\nabla_{\mathbf{x}}(\mathbf{q}(\mathbf{x}))^T] \dot{\mathbf{x}}} \\
 &\quad - f(\mathbf{x}) \sqrt{\dot{\mathbf{x}}^T \dot{\mathbf{x}}} \quad (6)
 \end{aligned}$$

where  $\dot{\mathbf{x}}^I = [\nabla_{\mathbf{x}}(\mathbf{q}(\mathbf{x}))^T]^T \dot{\mathbf{x}}$  transforms the tangent vector,  $\dot{\mathbf{x}}^I$ , at point  $\mathbf{x}^I$  of the  $\mathbf{x}_{\text{IRC}}^I$  curve into the image tangent vector,  $\dot{\mathbf{x}}$  at point  $\mathbf{x}$  on the  $\mathbf{x}_{\text{IRC}}$  curve. This relation is satisfied for each point on any IRC curve, and by extension on any SD curve, connecting points  $\mathbf{x}_0$  and  $\mathbf{x}_0^I$ . In Eq. 6 if we change  $\dot{\mathbf{x}}$  by  $\zeta \dot{\mathbf{x}}$ , which being  $\zeta$  either a positive or negative number, we obtain  $(\nabla_{\mathbf{x}} W(\mathbf{x}))^T \dot{\mathbf{x}} = 0$ , implying that,  $W = \text{constant} = W_0$ . With this result and Eq. 5, we have  $W(\mathbf{x}) - W_0 = 0 = (v^I - v_0^I) - (v - v_0)$ . Finally, the above relation between tangent vectors of both IRC curves gives the relation between gradient vectors of the PES at each point on those IRC curves:

$$\mathbf{g}(\mathbf{x}^I) = \dot{\mathbf{x}}^I = [\nabla_{\mathbf{x}}(\mathbf{q}(\mathbf{x}))^T]^T \dot{\mathbf{x}} = [\nabla_{\mathbf{x}}(\mathbf{q}(\mathbf{x}))^T]^T \mathbf{g}(\mathbf{x}) \quad (7)$$

Taking into account all the results obtained above, in the IRC model, we have a transformation of the coordinates,  $\mathbf{x}_{\text{IRC}}^I = \mathbf{q}(\mathbf{x}_{\text{IRC}})$ , that has the stigmatic character. In other words, integral (Eq. 1) evaluated from the reactant point to its image point, the product point, or vice-versa, is a constant equal to zero, because according to Eq. 5  $v_0 - v_0^I = -(v_0^I - v_0)$ , implying that  $v_0 = v_0^I$ . Furthermore, we can say that

$$\begin{aligned}
 \int_{t_0}^t F(\mathbf{x}_{\text{IRC}}^I, \dot{\mathbf{x}}_{\text{IRC}}^I) dt' &= \int_{t_0}^t F(\mathbf{x}_{\text{IRC}}, \dot{\mathbf{x}}_{\text{IRC}}) dt' \\
 &= (v^I - v_0^I) = (v - v_0) \quad (8)
 \end{aligned}$$

which tells us that the variation of the PES function,  $V(\mathbf{x}) - V(\mathbf{x}_0)$ , through an IRC curve (optical length of a ray path in GO), equals the variation through its image IRC curve. These results prove the formulation of Maxwell's theorem in the context of the IRC path theory.

Finally, we say that the transformation  $\mathbf{x}_{\text{IRC}}^I = \mathbf{q}(\mathbf{x}_{\text{IRC}})$  and  $\nabla_{\mathbf{x}} V(\mathbf{x}_{\text{IRC}}) = \mathbf{g}(\mathbf{x}_{\text{IRC}}) = [\nabla_{\mathbf{x}}(\mathbf{q}(\mathbf{x}_{\text{IRC}}))^T]^T \nabla_{\mathbf{x}} V(\mathbf{x}_{\text{IRC}}) = [\nabla_{\mathbf{x}}(\mathbf{q}(\mathbf{x}_{\text{IRC}}))^T]^T \mathbf{g}(\mathbf{x}_{\text{IRC}})$  is a canonical transformation of the variational problem under consideration, because it preserves the total differential form given in Eq. 5, with  $W$  being the generating function of this canonical transformation [7]. In particular, the transformation of the set of coordinates associated to a chiral structure should preserve this requirement if the IRC model is valid to describe its enantiomerization mechanism through narcissistic pathways.

The above canonical transformation applies to any narcissistic reaction independently if it proceeds through a synchronous (Fig. 1) or a nonsynchronous (Fig. 2) process. Nevertheless, in the first case, the application of the afore results leads to some particularities that are worth mentioning here. The MEP for a synchronous narcissistic reaction is described by a set of coordinates such that a subset of them are antisymmetric and become zero simultaneously at some point along the path [2]. The point where the antisymmetric coordinates become zero is in the mirror plane and this becomes the plane of symmetry for the reaction. The curve associated to the MEP thus passes through the mirror (see Fig. 1). According to the previous discussion, we take as a representation of this MEP an IRC curve that connects the points  $\mathbf{x}_0$  and  $\mathbf{x}_0^I$ , and the transformation  $\mathbf{x}_{\text{IRC}}^I = \mathbf{q}(\mathbf{x}_{\text{IRC}})$  is a linear transformation with respect to  $\mathbf{x}_{\text{IRC}}$ . In more detail,  $\mathbf{x}_{\text{IRC}}^I = \mathbf{Q} \mathbf{x}_{\text{IRC}}$ , where  $\mathbf{Q}$  is a matrix satisfying the reflection condition imposed by the mirror and being independent of  $\mathbf{x}$ . Since this IRC path goes through a mirror, there exists a point where  $\mathbf{x}_{\text{IRC}} = \mathbf{Q} \mathbf{x}_{\text{IRC}}$ , which means that a subset of coordinates becomes zero at this point of the IRC path. It is easy to see that due to the nature of matrix  $\mathbf{Q}$ , this subset corresponds to the antisymmetric coordinates. The point where  $\mathbf{x}_{\text{IRC}} = \mathbf{Q} \mathbf{x}_{\text{IRC}}$  must thus lie on the mirror. Applying Eq. 7 to this point, we obtain  $\dot{\mathbf{x}}_{\text{IRC}}^I = \nabla_{\mathbf{x}} V(\mathbf{x}_{\text{IRC}}) = \mathbf{Q}^T \nabla_{\mathbf{x}} V(\mathbf{x}_{\text{IRC}}) = \mathbf{Q}^T \dot{\mathbf{x}}_{\text{IRC}}$ , and this equality is satisfied only when  $\nabla_{\mathbf{x}} V(\mathbf{x}_{\text{IRC}}) = \mathbf{0}$ . With this result, we conclude that for synchronous narcissistic reactions the mirror must be necessarily located at a stationary point of the IRC path joining  $\mathbf{x}_0$  and  $\mathbf{x}_0^I$ . Since it lies on the mirror reflecting products and reactants, this stationary point must necessarily correspond to an achiral structure. We deduce thus from a strict application of the theory of CV that for synchronous narcissistic reactions, the point of the IRC path where the antisymmetric coordinates become zero must necessarily correspond to an achiral stationary point on this path.

### 3 Some illustrative examples: comparison of the enantiomerization mechanisms for [5]helicene and 1-hydroxy[4]helicene

All the calculations of the examples presented and discussed in this section were performed using the AM1 molecular orbital model and the UHF wave function [8]. This semiempirical method is, in our opinion, sufficient for our purposes, because in this work our interest is focused on the global features of the PES and not in a detailed description of the geometry and the energy of each individual configuration. Moreover, the AM1 method has been shown to be adequate to study the enantiomerization of  $[n]$ helicene compounds [9, 10]. The IRC path

was located employing the algorithm of González and Schelegel [11] as implemented in Gaussian [12] and GAMESS [13] codes.

Some enantiomerization rearrangements such that the transformation occurs through chiral pathways have been described in the literature (see, e.g., Ref. [14] and references therein). Recently, we have proposed such a mechanism for enantiomerization of 1-triptycyl[3]helicene [15], where the rotation of the triptycyl fragment is hindered by the [3]helicene fragment, which acts as a more or less stiff pawl. These two fragments are linked through a C–C bond that can be seen as an axle. Although the ideas exposed above may be applied to this example, to illustrate the concepts developed in the last section in a clear way, we will focus on a much simpler case and we will study the enantiomerization of [5]helicene as an example of synchronous narcissistic reaction and the enantiomerization of the related 1-hydroxy[4]helicene as an example for the nonsynchronous case. Visualization of the MEPs (represented by IRC curves) for these two rearrangements will be done using a reduced two-dimensional PES characterized by two antisymmetric coordinates that imply significant changes along the enantiomerization path. On one hand, each point on reduced two-dimensional PES has been obtained by minimizing the energy of the molecular structure considering the whole  $N$ -dimensional PES while freezing the two antisymmetric coordinates that have been chosen to define the two-dimensional PES. On the other hand, the IRC paths have been computed using the full  $N$ -dimensional PES and afterwards projected on the corresponding reduced two-dimensional PES. The two antisymmetric coordinates used in each case have been carefully chosen to force the projection of the IRC path to be a regular curve in the chosen two-dimensional subspace.

A convenient tool to highlight the different nature (chiral or achiral) of the enantiomerization paths for these transformations is to monitor the changes in chirality contents of the molecule along the reaction path using continuous chirality measures (CCM) [16–19]. The evaluation of the chirality content of an object (a molecular structure) described by a set of vertices requires finding the closest achiral structure. In the CCM formalism, this chirality contents is defined as the minimal distance that the vertices of the object (the nuclei in a molecule) have to be shifted to attain the desired achiral symmetry. Formally, given a chiral structure  $Q$  formed by  $M$  vertices with coordinates given by vectors  $\{\mathbf{q}_i\}_{i=1}^M$ , to calculate the CCM one must first find the set of vectors  $\{\mathbf{p}_i\}_{i=1}^M$  defining the nearest achiral structure. The CCM is then obtained as

$$\text{CCM}(Q) = \min_{\{\mathbf{p}_1, \dots, \mathbf{p}_M\}} \frac{\sum_{i=1}^M |\mathbf{q}_i - \mathbf{p}_i|^2}{\sum_{i=1}^M |\mathbf{q}_i - \mathbf{q}_0|^2} \times 100 \quad (9)$$

where  $\mathbf{q}_0$  is the position vector of the geometric center of the analyzed structure  $Q$ , the denominator is a mean square normalization factor, and the factor 100 is introduced for convenience. The bounds for the continuous chirality measure are  $0 \leq \text{CCM}(Q) \leq 100$ . If a structure is achiral, then  $\text{CCM}(Q) = 0$  and the CCM increases as its chirality content increases.

Let us now start our discussion by analyzing the enantiomerization process for the simpler case of [5]helicene (see Fig. 3). The minimum energy structure for this molecule corresponds to a nonplanar disposition of the five condensed benzene rings, which are angularly annulated resulting in a chiral helical staircase (clockwise or counterclockwise) as found in experimental studies [20]. The minimum in the PES,  $\mathbf{x}_0$ , and its mirror image,  $\mathbf{x}_0^1$ , correspond to these chiral helices structures. For this case, the transition state corresponds to a structure with  $C_s$  symmetry. The symmetry plane of this transition state structure is not the molecular plane for a hypothetical planar structure (let us name it as the *equatorial* plane) but an *axial* plane perpendicular to it (see Fig. 3). Although any mirror plane relating the two minima  $\mathbf{x}_0$  and  $\mathbf{x}_0^1$  can be used to analyze the reaction path for the enantiomerization using two antisymmetric coordinates, it is only using the symmetry plane of the transition state (if present) that it is possible to obtain a simple two-dimensional representation of this synchronous narcissistic reaction (as shown in Fig. 1). To illustrate this fact, we have used both the *axial* and the *equatorial* plane as a mirror plane to describe the enantiomerization process for [5]helicene. First of all, it is necessary to choose two antisymmetric coordinates for each of the selected planes. In Fig. 4, we define three internal coordinates for [5]helicene (three dihedral angles,

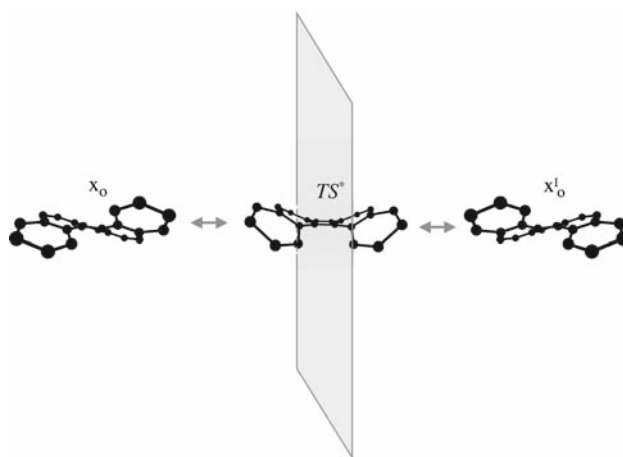


**Fig. 3** The enantiomerization of [5]helicene represented by the action of the symmetry plane, which is taken as a mirror plane. The two coordinates used to represent the two-dimensional reduced PES reported in Fig. 5 are antisymmetric with respect to this plane

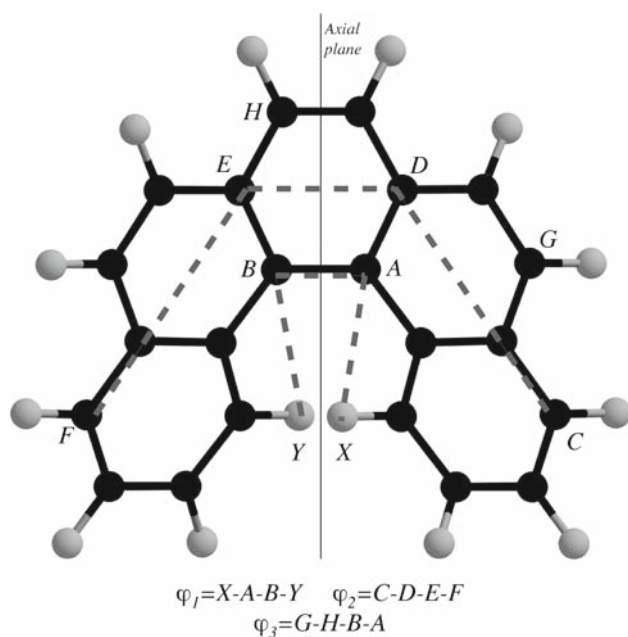


**Fig. 4** The two antisymmetric coordinates with respect the axial plane (dihedral angles  $\varphi_1$  and  $\varphi_2$ ) chosen to represent the two-dimensional reduced PES of [5]helicene (Fig. 5). The third coordinate (dihedral angle  $\varphi_3$ ) is not antisymmetric with respect the axial plane. All the three coordinates are antisymmetric with respect to the equatorial plane. When this latter is used as a mirror plane,  $\varphi_1$  and  $\varphi_2$  are chosen to represent the two-dimensional reduced PES (Fig. 11)

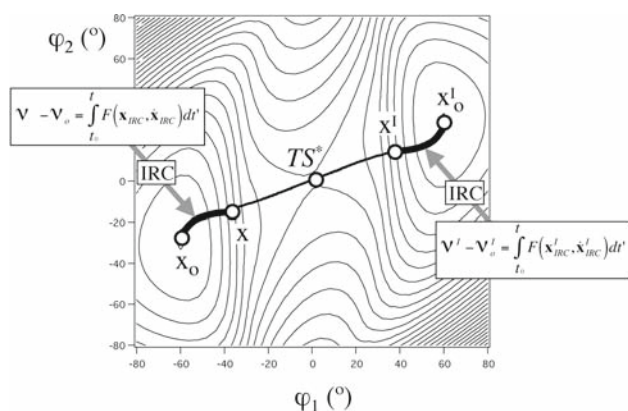


**Fig. 5** The reduced PES and the IRC path of the enantiomerization of [5]helicene described using an axial mirror plane to define the two antisymmetric coordinates  $\varphi_1$  and  $\varphi_2$  (given in Fig. 4). The *thin black lines* are the contour lines of the PES  $V(\mathbf{x}) = v$ . The *black line* is the IRC curve and the *flat black lines* are the subarcs of IRC curve that joins the points  $\mathbf{x}_0$  and  $\mathbf{x}$  and the corresponding image points  $\mathbf{x}'_0$  and  $\mathbf{x}'$ . In both subarcs, the “travel” potential energy is,  $v - v_0 = v' - v'_0$ . This potential energy difference coincides with the value of the integral (Eq. 1) evaluated along this subarc of the IRC curve. See text for more details

$\varphi_i$ ) including two antisymmetric coordinates with respect to the axial plane ( $\varphi_1$  and  $\varphi_2$ ) and two antisymmetric coordinates with respect to the equatorial plane ( $\varphi_1$  and  $\varphi_3$ ). The choice of these coordinates is arbitrary, because

any other pair of antisymmetric coordinates would lead to qualitatively similar results.

Let us start our analysis with the first choice, that is, we select the axial plane as the mirror relating reactants and products. The reduced PES with the projected MEP curve represented as the IRC path for the [5]helicene case using  $\varphi_1$  and  $\varphi_2$  to construct the reduced two-dimensional PES is shown in Fig. 5. The thin bold lines correspond to the contour lines of the reduced PES, while the bold line indicates the MEP connecting the two minima ( $\mathbf{x}_0$  and its mirror image  $\mathbf{x}'_0$ ). The heavier lines in Fig. 5 indicate the segment of the IRC curve joining the minimum energy configuration  $\mathbf{x}_0$  and an arbitrary point  $\mathbf{x}$  on the  $\mathbf{x}_{\text{IRC}}$  curve or points  $\mathbf{x}'_0$  and  $\mathbf{x}'$  on its image curve,  $\mathbf{x}'_{\text{IRC}}$ . For each pair of points  $\mathbf{x}'_{\text{IRC}}$  and  $\mathbf{x}_{\text{IRC}}$  on these two subarcs of the MEP, there is a relation  $\mathbf{x}'_{\text{IRC}} = \mathbf{Q} \mathbf{x}_{\text{IRC}}$ , with  $\mathbf{Q}$  having the following form

$$\mathbf{Q} = \begin{pmatrix} \mathbf{I}_{N-2} & \mathbf{0} & \mathbf{0} \\ \mathbf{0}^T & -1 & 0 \\ \mathbf{0}^T & 0 & -1 \end{pmatrix} \quad (10)$$

where  $\mathbf{I}_{N-2}$  is the unit matrix of dimension  $(N-2) \times (N-2)$ , and  $\mathbf{0}$  a zeroed vector of dimension  $N-2$ , with  $N$  being the number of internal coordinates (the dimension of the full PES; 102 for [5]helicene). The last two diagonal elements of matrix  $\mathbf{Q}$  are related to the antisymmetric coordinates that have been chosen to represent the reduced two-dimensional PES. Notice that  $\mathbf{Q}$  is independent of  $\mathbf{x}$ . It is easy to prove through Eq. 6 that the transformation,  $\mathbf{x}'_{\text{IRC}} = \mathbf{Q} \mathbf{x}_{\text{IRC}}$ , and,  $\mathbf{g}(\mathbf{x}'_{\text{IRC}}) = \mathbf{Q}^T \mathbf{g}(\mathbf{x}_{\text{IRC}})$ , where  $\mathbf{Q}$  is the matrix given in expression (Eq. 10), is canonical. In more detail, since  $\mathbf{Q}^T \mathbf{Q} = \mathbf{I}$  and  $\mathbf{Q}^T = \mathbf{Q}$ , where  $\mathbf{I}$  is the unit matrix in the  $N$  space, then

$$\begin{aligned} f(\mathbf{x}_{\text{IRC}}) &= \sqrt{\mathbf{g}^T(\mathbf{x}_{\text{IRC}}) \mathbf{g}(\mathbf{x}_{\text{IRC}})} = \sqrt{\mathbf{g}^T(\mathbf{x}_{\text{IRC}}) \mathbf{Q} \mathbf{Q}^T \mathbf{g}(\mathbf{x}_{\text{IRC}})} \\ &= \sqrt{\mathbf{g}^T(\mathbf{x}'_{\text{IRC}}) \mathbf{g}(\mathbf{x}'_{\text{IRC}})} = f(\mathbf{x}'_{\text{IRC}}) \end{aligned} \quad (11)$$

Applying the same algebraic manipulation to the term  $(\dot{\mathbf{x}}_{\text{IRC}}^T \dot{\mathbf{x}}_{\text{IRC}})^{1/2}$ , we obtain as desired that  $F(\mathbf{x}'_{\text{IRC}}, \dot{\mathbf{x}}'_{\text{IRC}}) = F(\mathbf{x}_{\text{IRC}}, \dot{\mathbf{x}}_{\text{IRC}})$ , for each pair of points  $\mathbf{x}_{\text{IRC}}$  and  $\mathbf{x}'_{\text{IRC}}$  on the IRC path. Because of the independence of  $\mathbf{Q}$  with respect to  $\mathbf{x}$  and to the fact that the IRC passes through the mirror plane characterized by  $\mathbf{Q}$ , there must be a point on the IRC curve satisfying  $\mathbf{x}_{\text{IRC}} = \mathbf{Q} \mathbf{x}_{\text{IRC}}$ , which implies that the coordinates used to represent the reduced PES must become zero at this point. Regarding the PES, the point where the antisymmetric coordinates become zero is just a first-order saddle point of the PES, denoted by TS, as was proved in the previous section. In addition, since the two antisymmetric coordinates become zero at the TS point, it must correspond to an achiral molecular structure. For this reason, in this case, the TS point must coincide with its

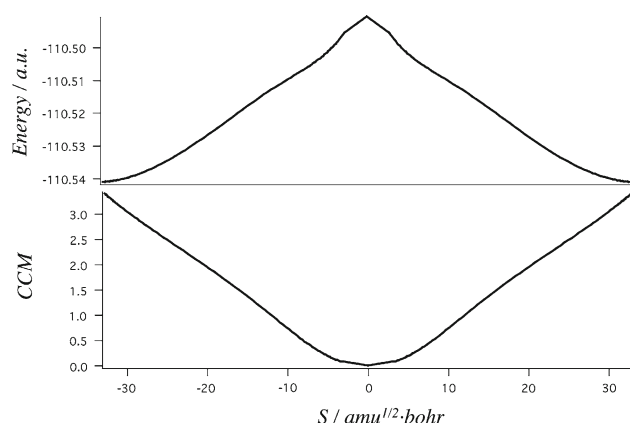


**Fig. 6** The AM1 energy and the chirality measure (CCM) along the IRC path for the enantiomerization of [5]helicene. Both values are symmetric with respect to the transition state ( $S = 0$ ), since the mirror image of each point in the left side ( $S < 0$ ) corresponds to a point of the IRC path in the right side ( $S > 0$ ). The transition energy ( $S = 0$  and maximum energy) also corresponds to a CCM minimum, since it is an achiral structure (CCM = 0)

image,  $TS^I$ . In other words, the IRC path passes through a mirror located at the TS point. It is interesting to analyze the variation of the energy and the chirality along the MEP (Fig. 6). It is easy to see that the enantiomerization proceeds via an achiral path (a path where there is at least one point for which CCM = 0) [18]. In this case, this achiral point coincides precisely with the achiral transition state that is denoted by  $TS^*$  in Figs. 3 and 5. Note also that in Fig. 6 both the variation of energy and CCM from the reactant to the transition state is the mirror image of the variation from the product to the transition state.

All these results show clearly that the enantiomerization of [5]helicene occurs by a narcissistic synchronous mechanism. Of course other SD curves linking  $\mathbf{x}_0$  and  $\mathbf{x}_0^I$  (without the category of the IRC one, that is, that do not include the transition state) may exist. These curves exhibit also the features described for the IRC, namely, each SD curve will have a point where the antisymmetric coordinates become zero; nevertheless, according to the reaction path (RP) model, these SD paths have no physical significance. If we consider, however, both the IRC and this set of SD paths joining points  $\mathbf{x}_0$  and  $\mathbf{x}_0^I$ , the resulting picture is then equivalent to that given by the propagation of light rays satisfying the requirements of a stigmatic transformation and Maxwell's theorem of GO. In other words, all these extremal paths, the set of SD paths plus the IRC one, emerging from point  $\mathbf{x}_0$  with PES value  $v_0$  and arriving to point  $\mathbf{x}_0^I$ , with PES value  $v_0^I$ , do not “enlarge the image,” since for all of them  $v_0 - v_0^I = 0$ .

Before using the equatorial plane as the mirror plane in the case of [5]helicene, let us analyze the example of the enantiomerization process for the related 1-hydroxy[4]helicene molecule (see Fig. 7), whose minimum energy

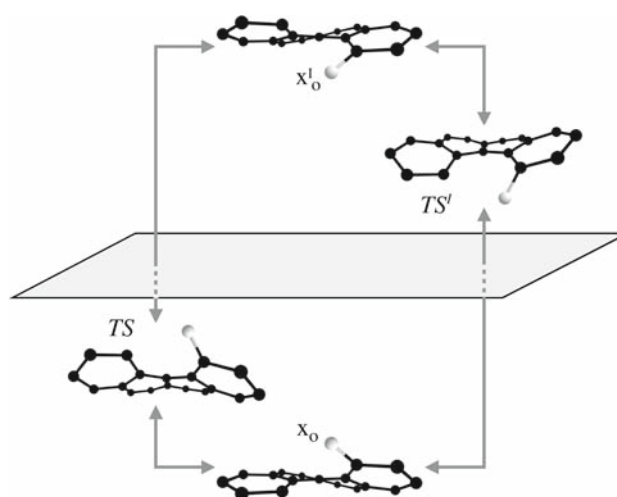


**Fig. 7** The enantiomerization of 1-hydroxy[4]helicene represented by the action of an equatorial mirror plane. The two coordinates used to represent the two-dimensional reduced PES reported in Fig. 9 are antisymmetric with respect to this plane

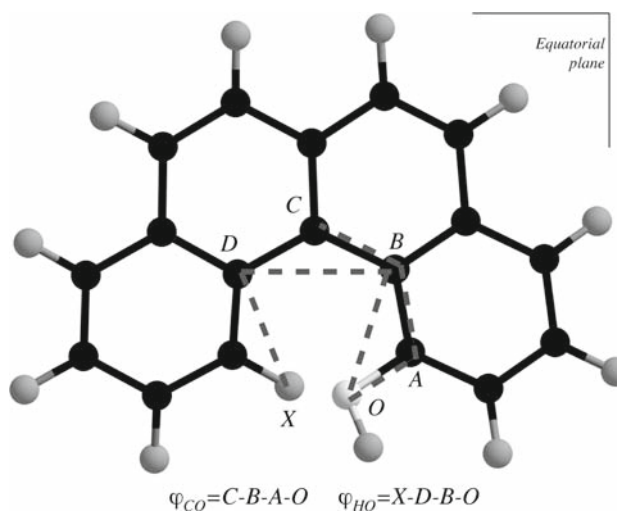


**Fig. 8** The two antisymmetric coordinates with respect to the equatorial plane (dihedral angles  $\varphi_{CO}$  and  $\varphi_{HO}$ ) chosen to represent the reduced PES of 1-hydroxy[4]helicene (Fig. 9)

structure is a chiral helical staircase (clockwise or counterclockwise) as found for [5]helicene. The enantiomerization process is however qualitatively different; in this case the enantiomerization does not proceed via any achiral structure, since no point of the reaction path (including the transition state) has a symmetry plane. Consequently, there is no preference for any specific mirror plane, and the *equatorial* plane has been chosen to define the antisymmetric coordinates, because it is the only one that could become a symmetry plane in a hypothetical planar structure (Fig. 7). The two antisymmetric coordinates (described in Fig. 8) have been selected to represent both the disposition (clockwise or counterclockwise) of the



full structure,  $\varphi_{\text{HO}}$ , and the relative position of the oxygen atom,  $\varphi_{\text{CO}}$ .

Regarding the two-dimensional reduced PES shown in Fig. 9, we can see that now we find two MEPs represented by IRC curves connecting reactants  $\mathbf{x}_0$  and products  $\mathbf{x}_0^1$  that correspond to the two minimum energy enantiomers of 1-hydroxy[4]helicene. For this case, none of these two paths contains a point such that the two antisymmetric coordinates go simultaneously to zero. According to Salem [2], the latter result is a sufficient condition to conclude that the enantiomerization occurs through a nonsynchronous narcissistic process. In this case, when applying the transformation  $\mathbf{x}_{\text{IRC}}^1 = \mathbf{Q} \mathbf{x}_{\text{IRC}}$ , the transformed point  $\mathbf{x}_{\text{IRC}}^1$  does not fall on the same IRC path that contains  $\mathbf{x}_{\text{IRC}}$ . Each point of the  $\mathbf{x}_{\text{IRC}}$  path has an image point in the  $\mathbf{x}_{\text{IRC}}^1$  path, and both paths are different having only the starting and the ending points ( $\mathbf{x}_0$  and  $\mathbf{x}_0^1$ ) in common. It is easy to see that there are no points of the MEP falling on the mirror, and for this reason, we find two different transition states  $\text{TS}$  and  $\text{TS}^1$  for the reaction:  $\text{TS}$  is the first-order saddle point for the  $\mathbf{x}_{\text{IRC}}$  path, whereas  $\text{TS}^1$  is the first-order saddle point for the  $\mathbf{x}_{\text{IRC}}^1$  path, but according to the results of the previous section we must have  $v_{\text{TS}} = v_{\text{TS}^1}^1$  and  $v_0 = v_0^1$ . These facts lead us to the conclusion that the two transition states  $\text{TS}$  and  $\text{TS}^1$  found for this reaction must be enantiomers. In other words, we have not found any point of the reaction path such that the equality  $\mathbf{x}_{\text{IRC}} = \mathbf{Q} \mathbf{x}_{\text{IRC}}$  was fulfilled.

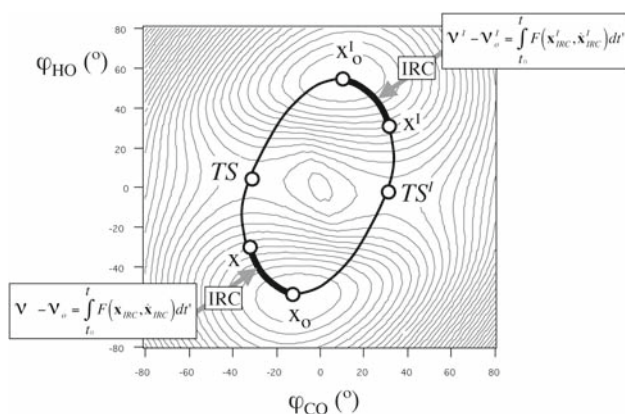


**Fig. 9** The reduced PES and the IRC path of the enantiomerization of 1-hydroxy[4]helicene. The description of the antisymmetric coordinates is as given in Fig. 8. The thin black lines are the contour lines of the PES,  $V(\mathbf{x}) = v$ . The black lines are the IRC curves connecting the minima points  $\mathbf{x}_0$  and  $\mathbf{x}_0^1$ , and the flat black lines are subarcs of these IRC curves. One of this subarc joint the points  $\mathbf{x}_0$  and  $\mathbf{x}$  and the corresponding image is the subarc that connects the points,  $\mathbf{x}_0^1$  and  $\mathbf{x}^1$ , and belongs to the image IRC curve. In both subarcs, the “travel” potential energy is,  $v - v_0 = v^1 - v_0^1$ . This potential energy difference coincides with the value of the integral (Eq. 1) evaluated along this subarc of the IRC curve. The total “travel” potential energy of each IRC curve coincides, which means that not “enlargement” of the energy potential is produced going from the point  $\mathbf{x}_0$  to  $\mathbf{x}_0^1$  or vice-versa. See text for more details

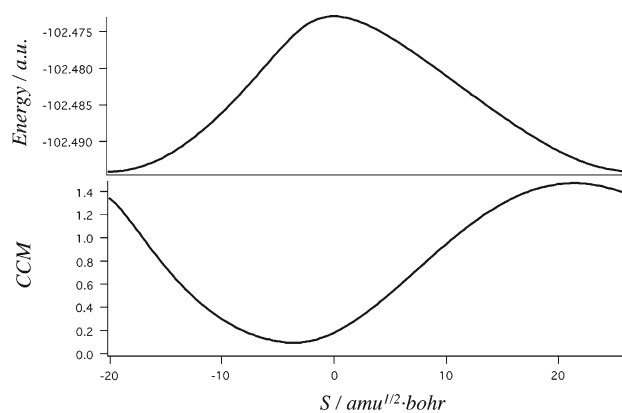


**Fig. 10** The AM1 energy and the chirality measure (CCM) along the IRC path for the enantiomerization of 1-hydroxy[4]helicene through the  $\text{TS}$  transition state (see Fig. 9). Curves are not symmetric with respect to the transition state ( $S = 0$ ). The mirror image of each point in this path corresponds to a point of the other IRC chiral path (through the  $\text{TS}^1$  transition state in Fig. 9). The transition energy ( $S = 0$  and maximum energy) does not correspond to a CCM minima and the CCM value never equals zero, since there is no achiral structure along this path

Nevertheless, we emphasize again that between the paths the relations  $\mathbf{x}_{\text{IRC}}^1 = \mathbf{Q} \mathbf{x}_{\text{IRC}}$  and  $v - v_0 = v^1 - v_0^1$  are satisfied at each point of the paths.

When analyzing the changes in the CCM along the two paths (Fig. 10), we find that in this case the enantiomerization proceeds via a pair of chiral paths (the CCM never drops to 0 along the path). Contrary to what was found for the former case, the changes in the CCM along each individual path do not show now the mirror symmetry around the transition states; it is however easy to see that the change in CCM when going from the reactant to the transition states; along one of the two paths is exactly the same as when going from the product to the transition state along the other path.

As in our other example, other SD paths emerging from point  $\mathbf{x}_0$  and arriving to point  $\mathbf{x}_0^1$  may exist on the full PES, and each one has an image SD curve associated with it, but as in the previous case, according to the RP model, it is not possible to assign any physical significance to this set of curves. Nevertheless, if one considers both types of paths together, the resulting picture of the PES is again equivalent to that given by the propagation of light rays moving through an isotropic medium satisfying the requirements of stigmatic transformation and Maxwell theorem [4]: the set of paths does not enlarge the “image” ( $v_0 = v_0^1$ ).

The fact of having a nonsynchronous mechanism for a narcissistic reaction is a necessary, but not sufficient, condition for finding a pair of chiral paths, since the two paths could reach an achiral point due to the existence of either a reflection plane different from that relating reactants and products chosen as the mirror plane or a higher order improper axis. To illustrate this point, let us come

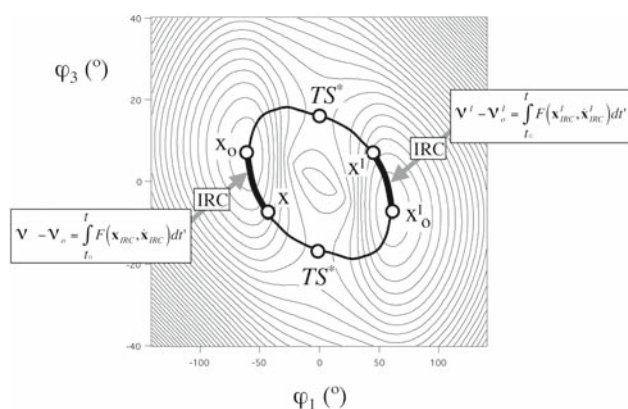


**Fig. 11** The reduced PES and the IRC path of the enantiomerization of [5]helicene described using an equatorial mirror plane to define the two antisymmetric coordinates  $\phi_1$  and  $\phi_3$  (given in Fig. 4). The thin black lines are the contour lines of the PES,  $V(\mathbf{x}) = v$ . The black lines are the IRC curves connecting the minima points  $\mathbf{x}_0$  and  $\mathbf{x}_0^I$ , and the flat black lines are subarcs of these IRC curves. One of this subarc joins the points  $\mathbf{x}_0$  and  $\mathbf{x}$  and the corresponding image is the subarc that connects the points,  $\mathbf{x}_0^I$  and  $\mathbf{x}^I$ , and belongs to the image IRC curve. In both subarcs, the “travel” potential energy is,  $v - v_0 = v^I - v_0^I$ . This potential energy difference coincides with the value of the integral (Eq. 1) evaluated along this subarc of the IRC curve. The total “travel” potential energy of each IRC curve coincides, which means that no “enlargement” of the energy potential is produced when going from the point  $\mathbf{x}_0$  to  $\mathbf{x}_0^I$  or vice versa. See text for more details

back to the enantiomerization of [5]helicene (Fig. 3). As shown before, if the symmetry plane of the transition state (the axial plane) is chosen as the mirror plane to define the coordinates describing the [5]helicene enantiomerization, the two-dimensional map of the reduced PES and the reaction path projection appears as a synchronous process (Fig. 5), with an achiral transition state in the origin of the antisymmetric coordinates axes. On the contrary, if any other plane is chosen (e.g., the equatorial plane) as the mirror plane (antisymmetric coordinates  $\phi_1$  and  $\phi_3$  defined in Fig. 4), the two-dimensional representation (Fig. 11) looks like that found in the case of 1-hydroxy[4]helicene (Fig. 9). However, as seen before, when analyzing the changes in the CCM along the reaction path (Fig. 6), it is clear that the enantiomerization proceeds via an achiral path (CCM equals zero for transition state and the variation of the CCM starting at the reactant is the mirror image of the variation of the CCM starting at the product). So, although in the map constructed using the equatorial mirror plane we apparently find two different transition states as in the case of 1-hydroxy[4]helicene, in fact, they both correspond to a single achiral transition state,  $TS^*$ . The dual projection in the two-dimensional PES for this  $TS^*$

raises from the fact that the coordinates used are not anti-symmetric with respect to its symmetry plane. In fact, these two points on this two-dimensional particular map are not only related by the mirror plane but also by a  $C_2$  rotation axis. We have included this example to show that a careful symmetry analysis is essential to choose the proper map for establishing the nonsynchronicity of a narcissistic reaction.

**Acknowledgments** Financial support from the Spanish *Ministerio de Ciencia y Tecnología*, DGI projects CTQ2005-08123-C02-01/BQU and CTQ2005-01117/BQU, and in part from the *Generalitat de Catalunya* projects 2005SGR-00036 and 2005SGR-00111 is fully acknowledged. M. L. gratefully acknowledges the *Ramón y Cajal Program*.

## References

1. Eliel EL, Wilen SH (1994) Stereochemistry of organic compounds. Wiley, New York
2. Salem L (1971) Acc Chem Res 4:322. doi:10.1021/ar50045a005
3. Fukui K (1981) Int J Quantum Chem Quantum Chem Symp 15:633
4. Luneburg RK (1944) Mathematical theory of optics, chap II. Brown University, Providence
5. Heidrich D (ed) (1995) The reaction path in chemistry: current approaches and perspectives. Kluwer, Dordrecht
6. Crehuet R, Bofill JM (2005) J Chem Phys 122:234105. doi:10.1063/1.1927521
7. Courant R, Hilbert D (1953) Methods of mathematical physics. Wiley, New York
8. Dewar MJS, Zoebisch EG, Healy EF, Stewart JJP (1985) J Am Chem Soc 107:3902. doi:10.1021/ja00299a024
9. Gimme S, Peyerimhoff SD (1996) Chem Phys 204:411. doi:10.1016/0301-0104(95)00275-8
10. Janke RH, Haufe G, Würthwein EU, Borkent JH (1996) J Am Chem Soc 118:6031. doi:10.1021/ja950774t
11. González C, Schlegel HB (1989) J Chem Phys 90:2154. doi:10.1063/1.456010
12. Frisch MJ, et al (2003) Gaussian03, Revision B.4. Gaussian Inc., Wallingford
13. Schmidt MW, Baldridge KK, Boatz JA, Elbert ST, Gordon MS, Jensen JH et al (1993) J Comput Chem 14:1347. doi:10.1002/jcc.540141112
14. Mauksch M, Schleyer PvR (1997) Angew Chem Int Ed 36:1856
15. Llunell M, Alemany P, Bofill JM (2008) Chemphyschem 9:1117. doi:10.1002/cphc.200800052
16. Avnir D, Zabrodsky Hel-Or H, Mezey PG (1998) In: Schleyer PvR (ed) Encyclopedia of computational chemistry. Wiley, New York
17. Zabrodsky H, Peleg S, Avnir D (1992) J Am Chem Soc 114:7843. doi:10.1021/ja00046a033
18. Pinto Y, Salomon Y, Avnir D (1998) J Math Chem 23:13. doi:10.1023/A:1019148619809
19. Alvarez S, Alemany P, Avnir D (2005) Chem Soc Rev 34:313. doi:10.1039/b301406c
20. Martin RH (1974) Angew Chem Int Ed 13:649